AD _ **405 851**_

DEFENSE DOCUMENTATION CENTER

FOR

SCIENTIFIC AND TECHNICAL INFORMATION

CAMERON STATION, ALEXANDRIA, VIRGINIA

63-3-5

RADC-TDR-63 149

15 March 1963

SOLID STATE MICROWAVE DELAY LINE

Final Technical Report

W. Brouillette

ELECTRONICS LABORATORY

GENERAL ELECTRIC COMPANY

SYRACUSE, NEW YORK

Contract No. AF30(602)-2230

Prepared for

ROME AIR DEVELOPMENT CENTER
RESEARCH AND TECHNOLOGY DIVISION
AIR FORCE SYSTEMS COMMAND
UNITED STATES AIR FORCE

GRIFFISS AIR FORCE BASE

RADC-TDR-63 149

15 March 1963

SOLID STATE MICROWAVE DELAY LINE
Final Technical Report

W. Brouillette

Electronics Laboratory
of the General Electric Company
Syracuse, New York

Contract No. AF30(602)-2230

Project No. 5578
Task No. 557802

Prepared
for
Rome Air Development Center
Research and Technology Division
Air Force Systems Command
United States Air Force

Griffiss Air Force Base
New York

i

TABLE OF CONTENTS

LIST OF ILLUSTRATIONS

Title of Report   RADC-TDR-63-149

Abstract

    Techniques for broadband generation of sound at microwave frequencies
have been developed. Using thin magnetostrictive film and a fine wire with
a broadband strip line, delay action was achieved over an 800 mcps band
from 1.1 gcps to 1.9 gcps. The theory of reflections and a detailed study
of appropriate modes in quartz is discussed, with a method of designing
a folded path delay line.

●

PUBLICATION REVIEW

This report has been reviewed and is approved.

Approved: *David F. Barber*
DAVID F. BARBER
Chief, Applied Research Laboratory
Directorate of Engineering
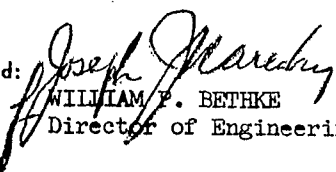
Approved: *Joseph Marechy*
WILLIAM P. BETHKE
Director of Engineering

FOR THE COMMANDER: *Irving J. Gabelman*
IRVING J. GABELMAN
Director of Advanced Studies

A. INTRODUCTION

This is a final report on work done by the Electronics Laboratory of the General Electric Company for the United States Air Force under Contract No. AF 30(602)2230. This report covers the period 15 January 1962 to 15 January 1963. The objective of this work is the formulation and application of design techniques for a microwave acoustic delay line.

During this report period, work has been concentrated in two major problem areas. These were: an investigation of techniques useful in achieving very wide bandwidth delay lines, with as low loss as possible, and techniques for designing folded path lines, in order to achieve longer delays by reflecting the signal several times in a block of delay medium. The high frequency involved makes it very difficult to achieve efficient coupling of electrical energy to mechanical energy and vice versa. These high frequencies and, hence, short acoustic wavelengths also make it necessary to use single crystals for delay media. Crystals of suitable materials are anisotropic and the usual designs for fused silica lines are not suitable.

In addition to these main areas, attention was devoted to testing of materials. This testing was done with the cooperation of personnel working on a concurrent program in phonon interactions in solids.

B. THIN FILM MATCHING TECHNIQUES

During the previous year, sound at microwave frequencies was success-
fully generated using electroplated films of nickel. This material is
magnetostrictive, and can be easily deposited in controlled manner by
electrodeposition. We have continued this work in the present period with
some success, and have developed a broad band structure that can be used to
excite such a film. In the present period we have used films formed from
electroplated alloys of nickel and iron and nickel and cobalt. These films
were prepared by first depositing a thin (ca. 100 AU) film of gold by
sputtering and then plating the magnetostrictive alloy from mixed solutions
with suitable electrodes. This work was done under the supervision of
Dr. I. W. Wolf of this laboratory.

The thin films have been convenient in testing transmission materials
other than quartz. The plated film is well bonded to the substrate, where-
as quartz transducers must be applied with some bonding agent such as indium
or grease, and much difficulty has been experienced with the latter. In
addition, the electromechanical coupling coefficient for bulk nickel is about
30% as compared to 9% for quartz, thus, theoretically one should be able to
achieve broader bandwidth with this material. It is easy to plate on a
film one-half sonic wavelength thick, for optimum transducer action.

In the first experiments with films, reported on in the first annual
report for this project, the films were excited in reentrant cavities, with
the delay rods enclosed in a hollow post. In more recent work, a much simpler
type of cavity has been used. A sketch of such a cavity is shown in
Figure 1. The cavity walls are fabricated of .020" wall stainless steel

2

tubing. Very thin end plates are turned of stainless steel, and the reentrant post is fitted to the center of one end. The post is made of stainless steel rod and is cut away at the root to enhance the AC magnetic field adjacent to the cut away section. The post is soldered into the bottom. The sample is inserted through a hole in the side near the base, so that the end bearing the film is nearly tangent to the post and can be held by clamps or cement.

Along the side of the cavity wall a slot permits the introduction of a coupling probe, which forms the terminus of the center conductor of a rigid coaxial 50 ohm transmission line. The line is made of thin wall stainless steel tubing, and has a saddle at the probe end in which the cavity can be clamped. A tuning screw of nylon or metal introduced through a threaded bushing over the end of the post allows limited adjustment of resonant frequency. The cavities can be made to cover the S-band (2-4 gcps) range in convenient sizes where the post is about 1/4 wavelength and for the L-band (1-2 gcps) range. An L-band cavity can be used at its third harmonic, where the post is approximately 3/4 wavelength. In some cavities of this type, peizoelectric quartz could be introduced into a hole directly over the post, and for tests, a large slot could be cut at the bottom end to insert a 1/4 inch slab with a film on one face close to the post. The cavities are very useful for helium tests, as they have a small heat capacity, and can be taken in and out of a cryostat without excessive heat loss to the helium.

The interior surfaces were well polished and silver plated to reduce cavity losses. These cavities show Q's of several thousand and thus have narrow bandwidths.

The narrow bandwidth of a cavity made it appear that some other matching device would be essential for a broadband delay line. The first attempt to accomplish this was the use of a thin wire as a short circuit at the receiving end of a transmission line. The film was placed so the wire was parallel to the film and as close as possible. This is shown in Figure 2. The end of the line is closed off by a cap, so the field is confined to the region near the fine wire. The structure was successful, and echoes were observed in X-cut quartz, at room temperature using a nickel-cobalt film to be described later. The wire forms a short circuit on the cable driving the structure, and large standing waves result, even with the use of a circulator, making it impractical to determine the available bandwidth. It was desired to test the feasibility of this arrangement for a delay line driver, so echo measurements were made using a transmitter, circulator and receiver at 1.3 gcps. A block diagram of the measurement apparatus is shown in Figure 3. To measure the input energy, an attenuator could be substituted for the circulator. After correcting for losses in the circulator, the insertion loss was 100 db for a delay of 4 microseconds between echoes. The use of a stub tuner to match the line to the transducer structure decreased the loss to 80 db. The loss in the material for this frequency and short delay is about 5-10 db, so most of this loss is due to mismatch.

In order to build a broad band structure of this type, it is necessary to compensate for the reflection at the junction of the coaxial line center conductor and the fine wire and to eliminate the reflection at the short.

4

In the structure shown in Figure 2 the fine wire acts like a short piece of transmission line of high impedance shorted on the far end.

The first approach to broad banding this structure was to try to use tapered lines, making a transition from 50 ohm line to a fine wire and back to 50 ohms, where a standard termination could be used. The fabrication of coaxial lines with tapered impedance appeared rather difficult, so strip line structures were resorted to.

These strip lines were constructed by using two parallel ground planes of aluminum, with a thin, brass strip symmetrically located as a center conductor. By varying the width and thickness of the strip, impedance can be changed easily. The spacing between ground planes was made so that standard type "N" connectors could be used as spacers and as terminals to join the strip line to ordinary coaxial lines.

In the first experiments, a fine silver wire .010" thick was used as a center conductor at the transducer. The ground planes were .250" apart, resulting in an impedance for the fine wire of about 200 ohms. The matching strips were made of brass .025" thick about one-half electrical wavelength lont at 1 gcps and tapered progressively from a width of .288" at the connector giving an impedance of 50 ohms to a width of .025" where the wire joined them giving an impedance of nearly 200 ohms. It was observed that the line showed a lower VSWR with one cover plate removed, at a frequency higher than the design frequency by almost a factor of two. This was analyzed as being due to the fact that at this freqeuncy the strip was about one-quarter wave long and the removal of the top raised the impedance of the matching section.

5

A better construction was then made, using two strips each one-quarter wave long at 1.5 gcps. The width of these strips was .083", yielding an impedance of 100 ohms, the geometric mean between 50 ohms and 200 ohms. A fine wire .002" in diameter and one-half wave long was placed between the strips. A diagram of this arrangement is shown in Figure 4. This assembly was mounted between type N connectors between two ground planes as shown in side vies in Figure 5. A hole was drilled in one of the ground planes so that a quartz crystal could be inserted with a thin film tangent to the fine wire.

One end of this structure was terminated in a 50 ohm resistor, and the VSWR looking into the other end was measured, and found to be 1.2 at center frequency. Putting a crystal in the hole raised the VSWR and gave irregular results for VSWR measurements, but echoes could be observed using a circulator and a short on the structure from 1.1 to 1.4 gcps. A photograph of these echoes at 1.2 gcps is shown in Figure 6.

In another experiment, the same line was filled with Teflon to minimize the discontinuity where the crystal is in proximity to the center wire. Although the standing wave measurements were improved somewhat, the ehco pattern was unchanged, so this was not photographed or pursued further.

An improved structure was built, using two lines parallel to one another, with one line for an input transducer and one line for an output transducer. A sketch of this arrangement is shown in Figure 7. With each of the transducer structures terminated, echoes were observed from 1.1 kMc to 1.9 kMc. A photograph of these echoes at 1.5 kMc is shown in Figure 8. This corresponds to a bandwidth of about 50% of center frequency, with a delay of four microseconds at room temperature.

6

The thin films used in the matching structure experiments were electroplated on a thin flash (ca. 100 AU) of gold deposited by sputtering on the polished ends of the quartz. An average composition of 5% cobalt-95% nickel was used, with a film thickness of 17,000 AU. This thickness was controlled by measuring the time and current density for deposition. In use an external bias field was applied to the films of some 1,000 - 2,000 gauss. The value of the necessary applied field depended on the particular sample being used. The variation in required field probably arises from several causes, the most effective one being the random domain orientation. There may be local variations in composition from the 5% - 95% average which would affect the characteristics. For some of the films, it was possible to magnetize them permanently by applying a 2,000 gauss field normal to the plane of the film and then switching off the magnet. The response of these permanently magnetized films is down 3-6 db from the response of the same film held in a bias field of the optimum value.

Insertion loss measurements for the wideband structure at 1.5 gcps was 100 db. This varied irregularly over the band from 1.1 gcps to 1.9 gcps, with $\pm$ 3 db to $\pm$ 6 db. The low signal level made the measurements open to some question, so at the band edges, 1.1 gcps and 1.9 gcps, the signal may have been down to 110 db. By substituting a fixed short for the 50 terminations on each line and using a stub tuner on each, the insertion loss could be reduced to 80 db, quite comparable to the results with a cavity, but the bandwidth was then about 5 mcps, indicating an effective Q of 200.

With this line, there was always severe feed through of the main pulse.
This was capacitive coupling between the metal films used for transducers.
Tight shields were fitted around the two lines to reduce the effects of
all other coupling, but this direct feed through was still severe. One
of the films was grounded to stop this unwanted coupling, but this reduced
the transmitted acoustic signal more than it reduced the feed through.
In a large block line, perhaps this could be minimized by careful location
of the transducers.

C. FOLDED PATH DELAY LINES IN ANISOTROPIC SOLIDS

A study of the problems inherent in the design of delays using long, folded paths with several reflections in a crystalline medium was carried out. The design problems are more difficult than those in isotropic media because the velocity of acoustic waves varies with the direction of travel in the medium. Further, the waves are no longer strictly longitudinal or shear waves. The most general motion of particles can be resolved into three orthogonal components, but these are not necessarily parallel or perpendicular to the wave front normal. Each of these three particle motion components will have its own phase velocity, and in general, all three phase velocities are different. Further, since the phase velocities vary with direction of the wave normal, the group velocity, or direction in which the energy is transported, will not be coincidnet with the phase velocity direction.

This report will use the notation adopted in Mason[1] for the propagation of waves in solid anisotropic media. These equations have been expanded and studied by Smyth[2] for the particular case of propagation in alpha quartz crystals. The treatment of reflection is rather complicated because of the variation of phase velocity with wave direction, and the design is further complicated because the energy flow direction does not coincide with the phase velocity.

The symmetry of the particular crystal used for a delay medium determines the variation of phase velocity with direction through its effect on the elastic constants, and each case has to be worked out in detail to

achieve a delay line design. We have worked out the case for quartz in some detail, and will present those results here. The basic equations are given in Mason and Smyth, and will only be recapitulated here for completeness, as they are rather lengthy.

Following Mason, we let the components of particle displacement along the x, y and z axes be u, v and w. The primitive equations of motion are, from Newton's second law:

$$\rho \, \frac{\partial^2 u}{\partial t^2} \quad dx \, dy \, dz \ = \ F_x$$

1)
$$\rho \, \frac{\partial^2 v}{\partial t^2} \quad dx \, dy \, dz \ = \ F_y$$

$$\rho \, \frac{\partial^2 w}{\partial t^2} \quad dx \, dy \, dz \ = \ F_z$$

The forces F_x, F_y, F_z are given in terms of the general stress strain tensor. If l, m, n are the direction cosines of the direction of propagation referred to the axes x, y and z, then s, the distance along the propagation path is given by:

2)
$$s = lx + my + nz$$

Upon substituting 2) into 1), and performing some manipulation, the general equations of motion become:

$$\rho \, \frac{\partial^2 u}{\partial t^2} \ = \ \lambda_{11} \frac{\partial^2 u}{\partial s^2} \ + \lambda_{12} \frac{\partial^2 v}{\partial s^2} \ + \lambda_{13} \frac{\partial^2 w}{\partial s^2}$$

3)
$$\rho \, \frac{\partial^2 v}{\partial t^2} \ = \ \lambda_{12} \frac{\partial^2 u}{\partial s^2} \ + \ \lambda_{22} \frac{\partial^2 v}{\partial s^2} \ + \ \lambda_{23} \frac{\partial^2 w}{\partial s^2}$$

$$\rho \, \frac{\partial^2 w}{\partial t^2} \ = \ \lambda_{13} \frac{\partial^2 u}{\partial s^2} \ + \ \lambda_{23} \frac{\partial^2 v}{\partial s^2} \ + \ \lambda_{33} \frac{\partial^2 w}{\partial s^2}$$

10

Where the quantities λ_{ij} are functions of the elastic constants of the particular medium and the direction cosines l, m, n as given by equation (A.40) in Mason.

Farnell[3] has made detailed theoretical studies of the propagation of waves in quartz and sapphire, which are both trigonal crystals. When the elastic constants of a trigonal crystal are substituted into equation (A.40) in Mason, then:

$$\lambda_{11} = l^2 c_{11} + m^2 \frac{c_{11} - c_{12}}{2} + n^2 c_{44} + 2mn c_{14}$$

$$\lambda_{22} = l^2 \frac{c_{11} - c_{12}}{2} + m^2 c_{11} + n^2 c_{44} - 2mn c_{14}$$

$$\lambda_{33} = l^2 c_{44} + m^2 c_{44} + n^2 c_{33}$$

4)
$$\lambda_{12} = lm \frac{c_{11} + c_{12}}{2} + 2ln\, c_{14}$$

$$\lambda_{13} = 2lm\, c_{14} + ln\, (c_{44} + c_{13})$$

$$\lambda_{23} = l^2 c_{14} - m^2 c_{14} + mn(c_{13} + c_{44})$$

Substituting expressions 4) into the equations of motion 3) yields equations in terms of the displacements parallel to the x, y, z axes, which of course are not the most suitable displacements to use. For a given direction, one can find linear combinations of u, v and w that yield three suitable wave eqautions. There are in general three distinct velocities for the three modes. As the direction is changed, the relative inclinations of the three mode directions to the direction of propagation changes.

11

Farnell has calculated the velocities of the three modes for varying direction in the three principal planes and plotted them in his paper. Smyth has also given the analytic expressions for the wave components in the three principal planes. The design of a line using arbitrary directions is enormously complicated, and the most likely approach is to examine the expressions in various planes and select those modes that can be used.

The design of a line using reflections can in principal be achieved using data from Smyth and Farnell, but it is necessary to understand the reflection conditions and the energy flow conditions very thoroughly. The design of reflecting lines in isotropic material is well understood, and the problem of mode conversion has been adequately treated. Additional complication arises when even a single mode upon reflection to a different direction now has a different velocity.

Suppose a plane wave approaches a plane surface with velocity C_1 and the angle the wave normal makes with the normal to the surface is θ_1, and let the same wave after reflection have velocity C_2 and let θ_2 be the angle of reflection measured as before. The relations are shown in Figure 9. The relation is given by:

5)
$$\frac{\sin \theta_1}{C_1} = \frac{\sin \theta_2}{C_2}$$

If upon reflection, a second mode can be generated, at velocity C_3, angle θ_3, then:

6)
$$\frac{\sin \theta_1}{C_1} = \frac{\sin \theta_2}{C_2} = \frac{\sin \theta_3}{C_3}$$

12

These relations are, of course, a generalized statement of Snell's law, which in optics is usually discussed for refraction at the interface between two isotropic media. In the present wave, the reflected wave behaves like a refracted wave because it sees a medium of different wave velocity after reflection. There is also the complication of the possible second polarization mode.

An examination of the propagation equations in quartz in the x-y, y-z and x-z planes reveals certain modes which should be useful for delay lines. One of them was briefly discussed by Smyth. In the course of this discussion, it will be necessary to gain an understanding of the effect of varying phase velocity magnitude on the actual direction of energy flow, since this must be clearly understood in order to design a multipath delay line.

This can be seen directly by considering the equations of motion for waves so oriented that the wave front normal always lies in the y-z plane. Following Smyth, these equation are:

$$\rho \frac{\partial^2 u}{\partial t^2} = \left(\frac{c_{11} - c_{12}}{2} \sin^2\theta + c_{44} \cos^2\theta + 2 c_{14} \sin\theta \cos\theta\right) \frac{\partial^2 u}{\partial s^2}$$

$$\rho \frac{\partial^2 v}{\partial t^2} = \left(c_{11} \sin^2\theta + c_{44} \cos^2\theta - 2 c_{14} \sin\theta \cos\theta\right) \frac{\partial^2 v}{\partial s^2}$$
$$+ \left[-c_{14} \sin^2\theta + (c_{44} + c_{13})\sin\theta \cos\theta\right] \frac{\partial^2 w}{\partial s^2}$$

$$\rho \frac{\partial^2 w}{\partial t^2} = \left[-c_{14} \sin^2\theta + (c_{44} + c_{13})\sin\theta \cos\theta\right]$$
$$+ \left(c_{44} \sin^2\theta + c_{33} \cos^2\theta\right) \frac{\partial^2 w}{\partial s^2}$$

13

In these expressions, θ is the angle between the wave front normal and the positive z axis. The first equation is a complete wave equation in u, the second pair constitute a coupled pair of wave equations, as Smyth points out. Physically, the first equation represents a wave whose particle velocity is always parallel to the x axis, that is to say a shear wave with the particle velocity always normal to the plane of propagation, which is the y-z plane. The second pair represent waves where particle motion is always in the plane of propagation, but whose components are not necessarily parallel or perpendicular to the axis of propagation.

If, in this system, we excite a plane wave whose particle motion is parallel to the x axis, and whose wave normal is parallel to the y-z plane, then it can travel in any direction in the y-z plane as a pure shear wave. Also, if it is reflected at any plane face which is parallel to the X axis, i.e. normal to the y-z plane, then the reflected wave will also be a shear wave with no mode conversion. Smyth has suggested the use of this mode as a delay line mode, and we have attempted to use it for a delay line.

A plot of the phase velocity of this mode is shown in Figure 10. This curve has been calculated from the elastic constants given in Farnell. Distance from the origin represents the magnitude of the phase velocity in the direction specified. Worthy of special interest are the directions for which the velocity shows maxima and minima. The velocity is maximum for a direction inclined about 35° to the z axis, and is minimum at about -55°, at right angles to the first direction. These are the directions of the BC and AC axes respectively, which are used for pure mode cuts in oscillator control crystals. When a wave travels along a direction for which its phase velocity is a maximum or minimum, the direction of energy flow coincides

14

with the direction of the wave normal.

An elegant treatment of the analogous case in optics in an anisotropic crystalline medium has been given by Born and Wolf.[4] The case for the optical medium is worked out for an uniaxial crystal such as quartz, and the results are almost identical, since the crystal symmetry has very similar effects on the elastic constants and the dielectric properties. For the particular case in question, the energy flow surface is an ellipse tangent to the phase velocity surface at the maxima and minima. The energy flow surface is the Huyghens surface used to express the laws of refraction and reflection in optics, and can be so used in the acoustic case. The most significant detail is that the energy flow direction coincides with the phase velocity direction for those directions where the phase velocity is maximum or minimum.

Since the mode under consideration can always be reflected from any plane parallel to the x direction without conversion, and shows a maximum and minimum in its phase velocity curve which are orthogonal to one another, it seems a likely candidate for a delay line. If such a line could be built, using crystalline quartz and arranging all the reflecting faces so that at each reflection, the direction is converted from that of the maximum to the minimum, or vice versa, then these directions can be used to determine the energy flow as well.

This same principle could be used to design a line using two directions of travel for any two modes that contain coincident energy flow and phase velocity directions.

In order to design such a line, it is necessary to determine the direction of reflecting planes that will reflect one mode onto the other. This can be illustrated by a calculation for the x shear waves propagating in the y-z plane. The equation for this mode is:

$$\rho \frac{\partial^2 u}{\partial t^2} = \left(\frac{c_{11} - c_{12}}{2} \sin^2\theta + c_{44} \cos^2\theta + 2 c_{14} \sin\theta \cos\theta\right) \frac{\partial^2 u}{\partial s^2}$$

$$= \left[\frac{c_{11} - c_{12}}{2} \left(\frac{1 - \cos 2\theta}{2}\right) + c_{44} \left(\frac{1 + \cos 2\theta}{2}\right) + c_{14} \sin 2\theta\right] \frac{\partial^2 u}{\partial s^2}$$

8)

$$= \left[\left(\frac{c_{11}}{4} - \frac{c_{12}}{4} + \frac{c_{44}}{2}\right) + \left(\frac{c_{44}}{2} + \frac{c_{12}}{4} - \frac{c_{11}}{4}\right)\cos 2\theta\right.$$

$$\left. + c_{14} \sin 2\theta\right] \frac{\partial^2 u}{\partial s^2}$$

The values of the elastic constants, taken from Farnell's paper, are:

$$c_{11} = .8694 \times 10^{11} \text{ newtons/m}^2$$
$$c_{44} = .5762 \qquad \text{"}$$
$$c_{12} = .0696 \qquad \text{"}$$
$$c_{14} = .1743 \qquad \text{"}$$
$$\rho = 2650 \text{ kg/m}^3$$

From these values,

9) $$10^{-11} \rho \frac{\partial^2 u}{\partial t^2} = (.48805 + .08815 \cos 2\theta + .1743 \sin 2\theta)\frac{\partial^2 u}{\partial s^2}$$

$$= (A + B \cos 2\theta + c \sin 2\theta) \frac{\partial^2 u}{\partial s^2}$$

hence

$$10^{-11} \rho c^2 = A + B \cos 2\theta + C \sin 2\theta$$

16

where c = velocity in direction θ from z axis. To find directions of maximum and minimum velocity:

10) $\frac{\partial}{\partial\theta}$ (A + B cos2θ + Csin2θ)= -2 Bsin2θ + 2 Csin2θ = 0

whence: tan 2 θ = $\frac{C}{B}$

for maximum θ is 31° 35' 11"

for minimum θ is - 58° 24' 49"

let C_M be the maximum velocity, and C_m be the minimum velocity

C_M = 5147 m/sec.

C_m = 3368 m/sec.

Now we derive an expression for the direction of a reflecting plane which will reflect a ray traveling in one of these directions to the other perpendicular direction. Let a ray traveling in the direction of maximum velocity strike such a reflecting plane at angle of incidence α, and leave at angle β, so that $\alpha + \beta = \pi/2$, Figure 11.

From the reflection condition:

$$\tan\alpha = \frac{C_M}{C_m} = \frac{5147}{3368}$$

11) α = 56° 47' 44"

β = 33° 12' 16"

Figures 12 and 13 show the constructions for each case. In Figure 12 a dotted ray from the origin of the y-z axes is drawn in the direction 31° 35' 16" for the direction of maximum velocity. The plane A-A intercepts this ray so its normal makes an angle of 56° 47' 44" in the sense

17

indicated. The projection of A-A will intercept the z axis at - 1° 37' 05".
In Figure 13, a plane A-A has a normal which intercepts the maximum
velocity direction at 56° 47' 44" in the opposite sense. In this case,
the plane A-A intercepts the z axis with an angle of 64° 47' 27".

Hence, if a delay line were fabricated from single crystal quartz
where all the reflecting surfaces were parallel to these two directions,
and a shear wave with the particle motion parallel to the x axis were used,
then the waves could be reflected at each face from one to the other of the
two directions for which energy flow is parallel to the wave front normal
and the path of the ray could be easily computed. There would, in this
case, be no mode conversion upon reflection. Energy could be delivered to
the sending end of the delay line and removed at the receiving end by
using shear transducers properly oriented on facets cut perpendicular to
the two directions. Thin films with drive wires and bias field properly
oriented could also be used.

An examination of the other modes involving propagation in planes
parallel to the xyz axes discloses at least one other set that should be
useful and which also involve particle displacement parallel to the x axis.

The equations of motion for propagation in the x-y and x-z planes
are given incorrectly in Smyth's report. We reproduce them correctly here.

18

In the x-y plane, let θ be the angle measured from the x axis to the normal, lying in that plane, then:

$$\rho \frac{\partial^2 u}{\partial t^2} = (c_{11} \cos^2\theta + \frac{c_{11} - c_{12}}{2} \sin^2\theta) \frac{\partial^2 u}{\partial s^2} + \frac{c_{11} + c_{12}}{2} \sin\theta \cos\theta \frac{\partial^2 v}{\partial s^2}$$
$$+ 2 c_{14} \sin\theta \cos\theta \frac{\partial^2 w}{\partial s^2}$$

$$\rho \frac{\partial^2 v}{\partial t^2} = \frac{c_{11} + c_{12}}{2} \sin\theta \cos\theta \frac{\partial^2 u}{\partial s^2} + (\frac{c_{11} - c_{12}}{2} \cos^2\theta + c_{11} \sin^2\theta) \frac{\partial^2 v}{\partial s^2}$$
12)
$$+ (c_{14} \cos^2\theta - c_{14} \sin^2\theta) \frac{\partial^2 w}{\partial s^2}$$

$$\rho \frac{\partial^2 w}{\partial t^2} = 2 c_{14} \sin\theta \cos\theta \frac{\partial^2 w}{\partial s^2} + (c_{14} \cos^2\theta - c_{14} \sin^2\theta) \frac{\partial^2 v}{\partial s^2} + c_{44} \frac{\partial^2 w}{\partial s^2}$$

In the x-z plane, let θ be the angle measured from the z axis to the normal, then:

$$\rho \frac{\partial^2 u}{\partial t^2} = (c_{11} \sin^2\theta + c_{44} \cos^2\theta) \frac{\partial^2 w}{\partial s^2} + 2c_{14} \cos\theta \sin\theta \frac{\partial^2 v}{\partial s^2}$$
$$+ (c_{44} + c_{13}) \sin\theta \cos\theta \frac{\partial^2 w}{\partial s^2}$$

$$\rho \frac{\partial^2 v}{\partial t^2} = 2c_{14} \cos\theta \sin\theta \frac{\partial^2 w}{\partial s^2} + (\frac{c_{11} - c_{12}}{2} \sin^2\theta + c_{44} \cos^2\theta) \frac{\partial^2 v}{\partial s^2} + c_{14} \sin^2\theta \frac{\partial^2 w}{\partial s^2}$$

13)

$$\rho \frac{\partial^2 w}{\partial s^2} = (c_{44} + c_{13}) \cos\theta \sin\theta \frac{\partial^2 u}{\partial s^2} + c_{14} \sin^2\theta \frac{\partial^2 v}{\partial s^2}$$
$$+ (c_{44} \sin^2\theta + c_{33} \cos^2\theta) \frac{\partial^2 w}{\partial s^2}$$

19.

The equations in the x-y plane offer the possibility of a suitable delay line mode by using directions for which the x component of displacement is one of the natural displacement directions. Along the x direction, θ is zero and u, the x component of displacement is a longitudinal wave. Along the y direction, $\theta = \pi/2$, and u represents a pure shear mode. From the Farnell paper, it is seen that these are both pure mode directions.

Thus, for $\theta = 0$

14)
$$\rho \frac{\partial^2 u}{\partial t^2} = c_{11} \frac{\partial^2 u}{\partial s^2}$$
$$\rho \frac{\partial^2 v}{\partial t^2} = \frac{c_{11} - c_{12}}{2} \frac{\partial^2 v}{\partial s^2} + c_{14} \frac{\partial^2 w}{\partial s^2}$$
$$\rho \frac{\partial^2 w}{\partial t^2} = c_{14} \frac{\partial^2 v}{\partial s^2} + c_{44} \frac{\partial^2 w}{\partial s^2}$$

For $\theta = \pi/2$

15)
$$\rho \frac{\partial^2 w}{\partial t^2} = \frac{c_{11} - c_{12}}{2} \frac{\partial^2 u}{\partial s^2}$$
$$\rho \frac{\partial^2 v}{\partial t^2} = c_{11} \frac{\partial^2 v}{\partial s^2} - c_{14} \frac{\partial^2 w}{\partial s^2}$$
$$\rho \frac{\partial^2 w}{\partial t^2} = -c_{14} \frac{\partial^2 v}{\partial s^2} + c_{44} \frac{\partial^2 w}{\partial s^2}$$

These solutions show the trigonal symmetry for rotation about the z axis, so there is a great amount of freedom in choosing the orientation of a block. There are three equivalent x axes and three y axes normal to these.

The two modes are at right angles one to another. The motion parallel to the x axis is a longitudinal mode and can be launched through the piezoelectric effect in the quartz itself by applying the oscillating field normal to a face cut in the right direction.

It is necessary to calculate the reflection angles for conversion of the x axis longitudinal wave into the y axis shear wave. Since the other modes are both orthogonal to the desired motion, there should be no conversion upon reflection.

The velocity along the x direction is given by $\left(\dfrac{c_{11}}{\rho}\right)^{\frac{1}{2}}$, and along the y direction by $\left(\dfrac{c_{11} - c_{12}}{\rho}\right)^{\frac{1}{2}}$.

Denoting the former by V_1 and the latter by V_S

$$V_1 = 5.708 \times 10^3 \text{ m/sec.}$$

$$V_S = 3.885 \times 10^3 \text{ m/sec.}$$

These are the well-known longitudinal velocity along the x axis and the slow shear velocity along the y axis.

In Figure 14 we show a diagram of the reflection condition. The longitudinal wave impinges on a reflecting surface at angle $\emptyset_1$ and is reflected at $\emptyset_S$.

From the reflection condition,

16) $\qquad \dfrac{v_1}{\sin\phi_1} = \dfrac{v_S}{\sin\phi_S} = \dfrac{v_S}{\cos\phi_1} \qquad\qquad \tan\phi_1 = \dfrac{v_1}{v_S}$

$$\emptyset_1 = 55^{\circ}51'16''$$

$$\emptyset_S = 90^{\circ} - \emptyset_1 = 34^{\circ}8'44''$$

The longitudinal wave travels parallel to the x axis and the shear wave parallel to the y axis.

Delay line blocks were cut and polished to test the possibility of using each of these modes. To test the x-shear mode in the y-z plane, a rather complicated block was designed. It is shown in Figure 15.

The face along AD is cut normal to the fast shear direction so that a wave generated on this face by a transducer will travel in the fast shear direction until it encounters either face AB or BC. At either of these faces it should be reflected through a right angle. Signals leaving face BC will always strike face AB and be returned to face AD where they could be detected. Signals leaving AB can strike either DC or BC. The block was so proportioned that signals could be used on either of the dotted paths, allowing 4 reflections or two reflections. Since AB was normal to the fast direction, reflections could return the signal on itself to the original input. Two of these blocks were cut and polished by Dell Optics from a single crystal of Sawyer Research Products quartz furnished by Rome Air Development Center. Extensive trials at room temperature and helium temperature were made on each using films bonded to the proper areas, but no signals could be observed. It was suggested that the material might show excessive attenuation, so a test was made using a film on face DC on one of the samples. With a cut away cavity of the type previously described, echoes could be observed which propagated between DC and AB. Three modes corresponding to the longitudinal, and the two shear modes for y-axis propagation were present. These were observed at about 90 db loss at room temperature. We are still at a loss in explaining why no propagation could be observed in the short path involving only two reflections. The directions of the crystal were checked by X-ray diffraction and were correct.

A simpler test block was made to test the pair of modes along the x and y axes. A right prism was cut to the shape shown in Figure 16, with the hypotenuse in the proper direction to reflect from one of the pure mode axes to the other. Time did not permit having this done by an outside firm,

so it was cut and polished in our machine shop. Control of the angles and flatness was not as precise as in the other case. This sample was also tested at room temperature and at helium temperature unsuccessfully. Perhaps in this case errors in orientation and angles were sufficient to impair correct operation.

D. MATERIALS

Some tests have been made on other materials available in single crystal
form. Polished crystals of silicon with thin films of nickel cobalt were
used to propagate sound at L band and S band in liquid helium. Several tens
of echoes can be observed, with severe modulation of the pattern due to
face misalignment making material loss measurements rather inaccurate. The
material loss is approximately .6 db/cm. Figure 17 shows a series of echoes
in <111> silicon at 2.27 gcps. The obscuring effects of the modulation
envelope are plainly seen. Very similar results are obtained in germanium.

A crystal of gallium arsenide was tested at 1.15 gcps, and about five
echoes were observed at 4° K. The propagation was along the <110> axis,
the mode was the fast shear mode. This orientation has the particle dis-
placement along the direction of peizoelectric activity, for possible use
as an electron-phonon interaction amplifier. The dimensions of the crystal
were 5 mm by 5 mm in cross-section and 1.5 cm long.

Light from a tungsten lamp focused on the sample caused the echoes to
decrease by a factor of about five in power. Since the light had to be
transmitted through a long narrow tube into the cryostat, a measure of
actual intensity at the sample could not be obtained. A field of 200 volts/
inch was applied along the propagation axis with the illumination applied.
The echoes increased to about one third of the original magnitude. The crystal
heated up rapidly so that a series of measurements at various values of
field intensity could not be obtained. We were unable to get similar results
from a pulsed experiment, but this experiment indicates a possibility of
amplification at frequencies over 1 gcps. A photograph of the echo pattern

under the three conditions of dark, light on, and both light and field on

appears in Figure 18.

A sample of very homogeneous ruby 2 cm long, prepared for use as a laser

crystal was tested. This crystal had end faces very finely polished for

optical applications. Propagation was along the C-axis. A thin film of

nickel cobalt was used and three echoes were observed at room temperature

at 3 gcps. A photograph of this echo pattern is reproduced in Figure 19.

The modulation pattern makes it impossible to obtain a reasonable estimate

for material losses, but the presence of a discernable signal at room

temperature indicates the losses must be considerably smaller than those

for quartz. Ruby has the same structure as quartz, and the possible modes

for a reflection line in quartz could be used in ruby or sapphire. The

availability of large blocks of ruby or sapphire would offer very interesting

possibilities for a delay line at room temperature.

E. CONCLUSIONS

The various measurements and experiments on broad band transducer structures indicate that the achievement of very low insertion losses is very difficult at microwave frequencies without some active internal amplification, such as might be available from electron-phonon or phonon-phonon amplifiers.

There is a fundamental problem of impedance matching between the very high effective impedance of a piezoelectric crystal or the very low effective impedance of a magnetostrictive device and the 50 ohm level of the signal circuits. The use of high Q cavities can multiply the effective fields by large factors, but the small sonic wavelengths at these frequencies demand an energy density which is very hard to achieve. The use of a cavity also restricts the bandwidth of a device. A possible alternative approach is to design transmission systems with very small dimensions so that the transducer would fill the entire cross-section, but this is very likely to be completely impractical.

The most likely alternative to this approach might be the use of yttrium iron garnet (YIG). At the beginning of this work, large single cyrstals of YIG were not available, but recently, these are becoming more easily obtained. YIG offers the possibility of very efficient transformation between electrical and mechanical energy, through the use of spin-wave phonon coupling, and some YIG samples are reported to have very low sonic losses at room temperature.

The use of YIG transducers with a large block of a single crystal medium such as quartz or the use of a large block of YIG could lead to a long delay line. If YIG must be used in conjunction with another material, then

a serious study and development of bonding methods will be necessary.

The failure of the present experiments to verify the theoretical study on reflections is not satisfying, but the theory is so well-founded and complete that these experiments can by no means be said to have negated the conclusions. There were no unjustified assumptions, and it is highly probable that more extensive experiments will bear out the mathematical conclusions.

The effects of anisotropy on propagation are very complicated, and the physical meaning of the equations of motion are obscured by the complexity of the mathematical equations, but it is very clear that it should be possible to build delay lines using anisotropic solids. We are confident that an understanding of the geometrical dispersion which causes the energy flow direction to fail to coincide with the phase normal direction will make it possible to design successful folded path lines, and it seems likely that the approach outlined here of seeking those modes where the phase and group velocities are coincident, with careful attention to reflection conditions will lead to successful construction of folded path lines in single crystals. We remark in passing that obviously this approach is applicable to the design of lines at lower frequencies as well, if the application of single crystal material seems to be desireable.

REFERENCES

1. W. P. Mason, "Physical Acoustics and the Properties of Solids,"
   D. Van Nostrand, Princeton, 1958.

2. H. T. Smyth, "Single Crystal Ultrasonic Delay Line Study," Final
   Report, Appendix, Contract AF30(602)-2051, Report RADC TR-60-157,
   ITT Laboratories, N.J., 1960.

3. G. W. Farnell, Can. J. Phys., $\underline{39}$, 65, (1961).

4. M. Born and E. Wolf, "Principles of Optics," p. 670 et seq, Pergammon
   Press, New York, 1959.
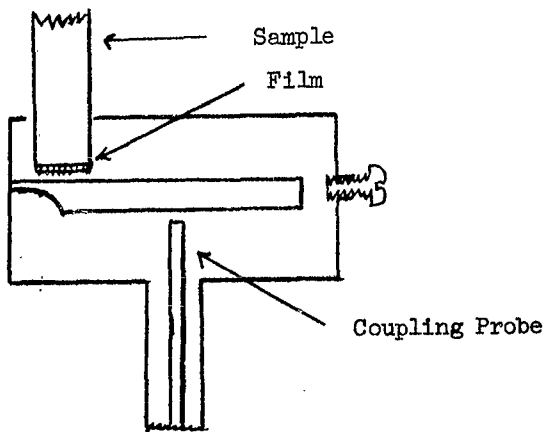
Figure 1. Testing Cavities for Films
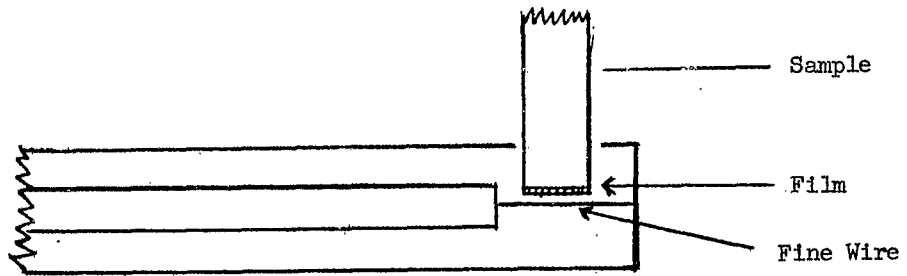
Figure 2. Shorted Fine Wire Structure
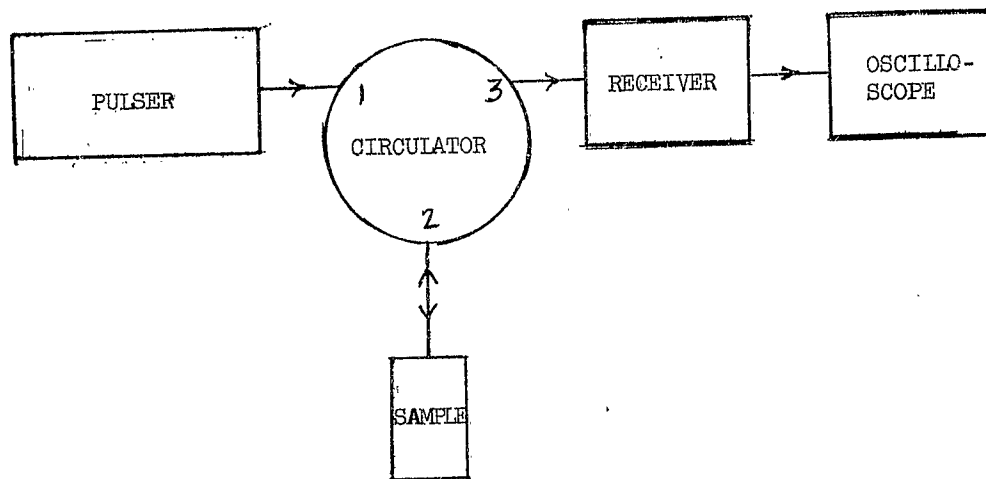
Figure 3. Block Diagram of Test Setup
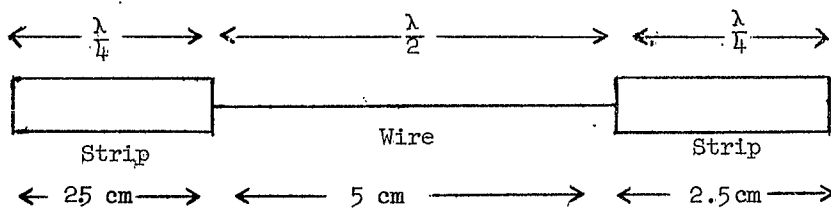
Figure 4. Fine Wire and Matching Strip
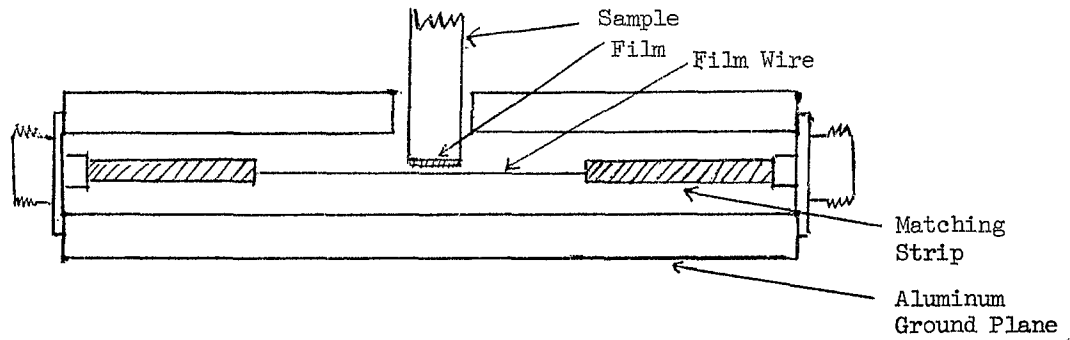
Figure 5. Broadband Strip Line Matching Structure
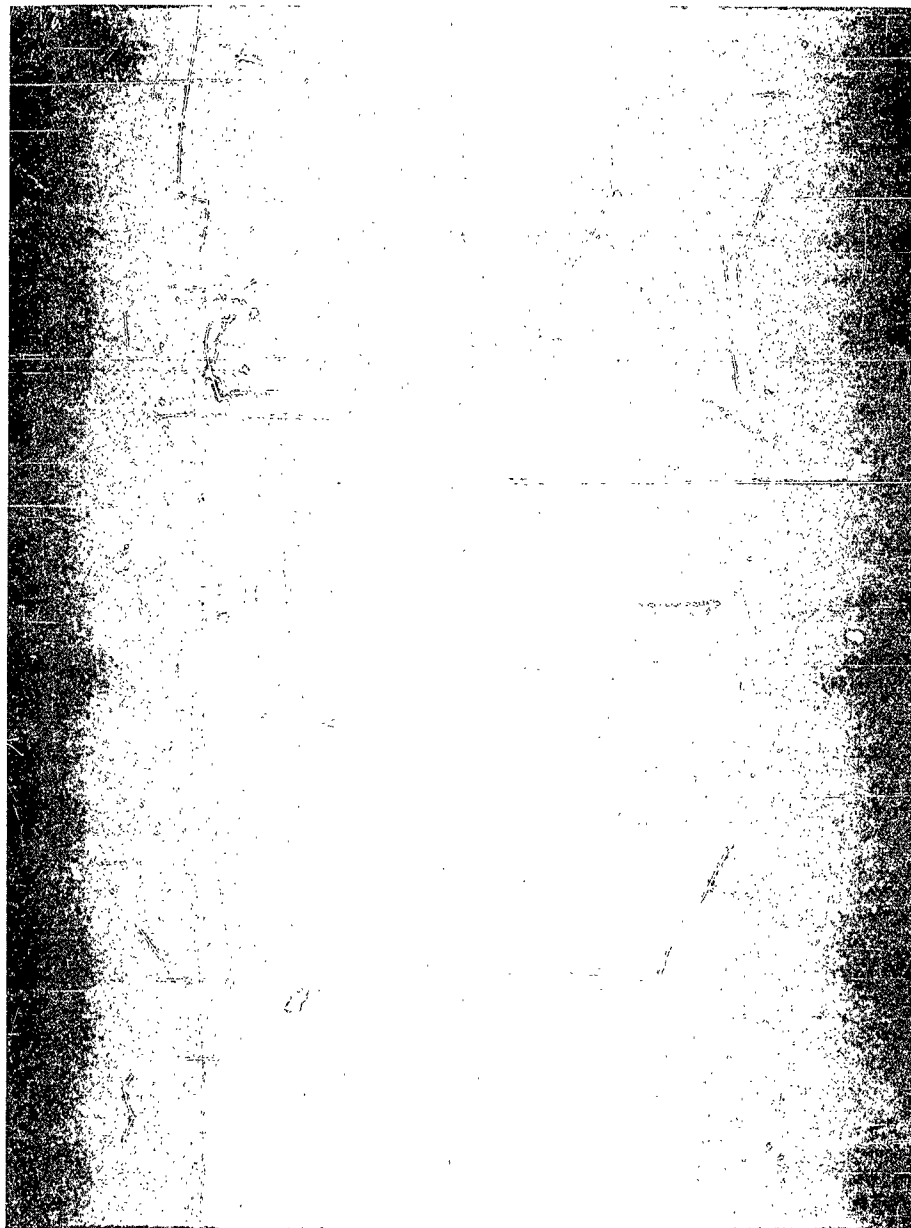
Fast Shear Mode in x cut Quartz
5 μsec/cm

Figure 6.   Echoes at 1-2 gcps in Shorted Fine Wire Driver Structure
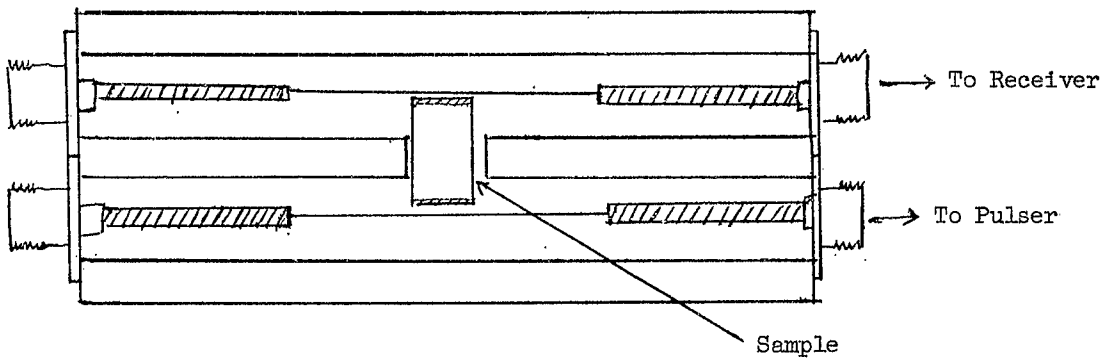
Figure 7. Double Matching Structure
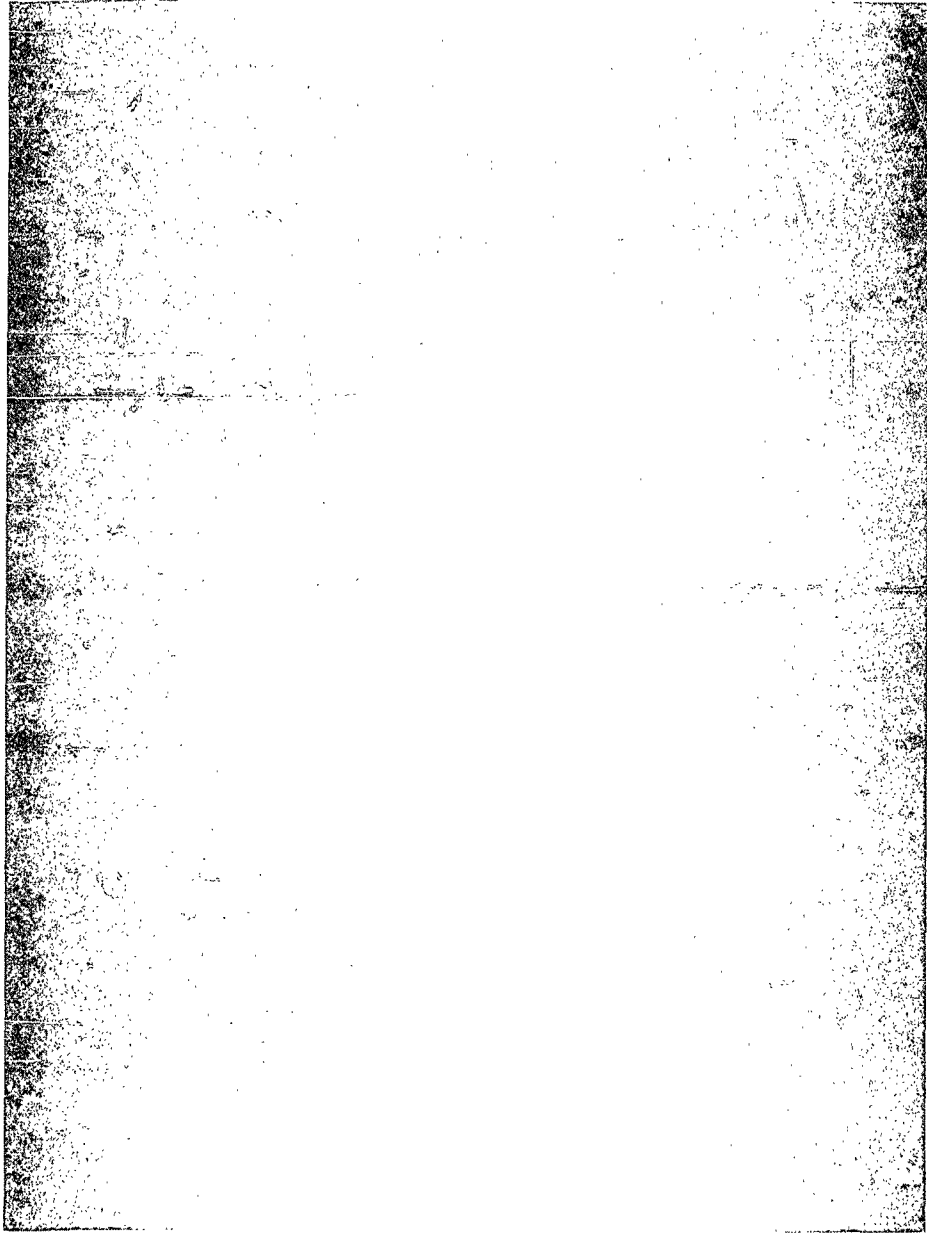
Fast Shear Mode in x cut Quartz
5 μsec/cm

Figure 8. Echoes at 1-5 gcps in Wideband Terminated Fine Wire Driver Structure
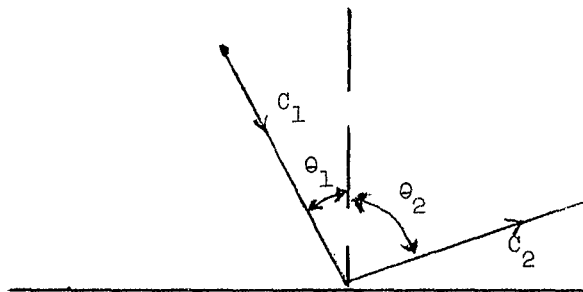
Figure 9. Reflection Geometry
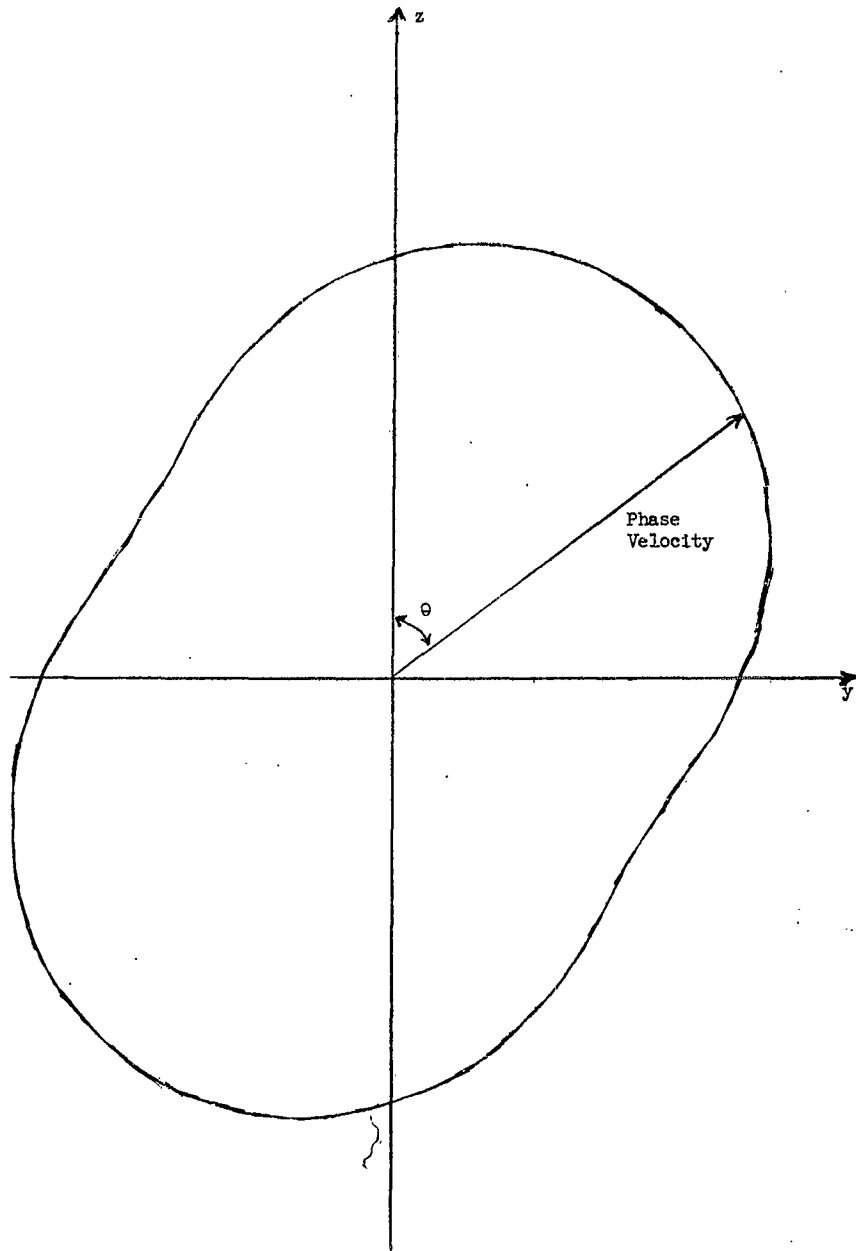
Figure 10. Phase Velocity of x-shear Mode
in y-z Plane in Quartz
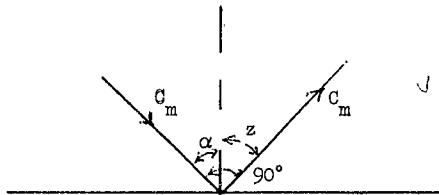
Figure 11. Reflection for x-shear Mode
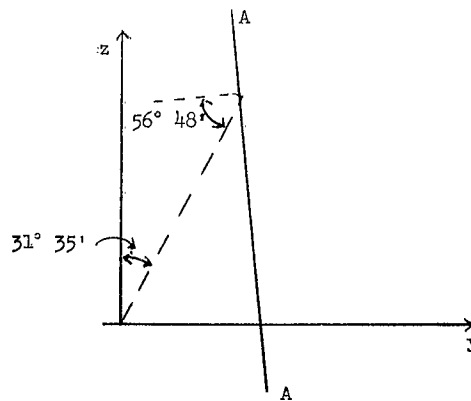
Figure 12. Reflection Geometry for x-shear Mode – 1st case
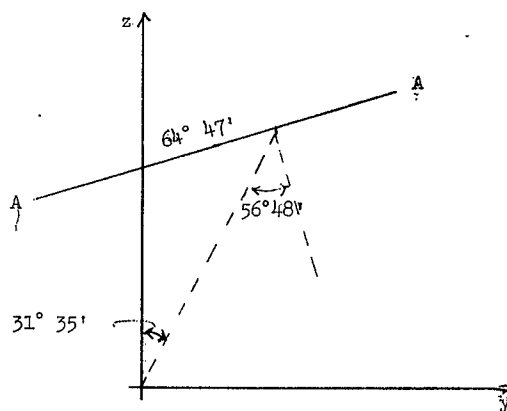
Figure 13. Reflection Geometry for x-shear Mode – 2nd Case
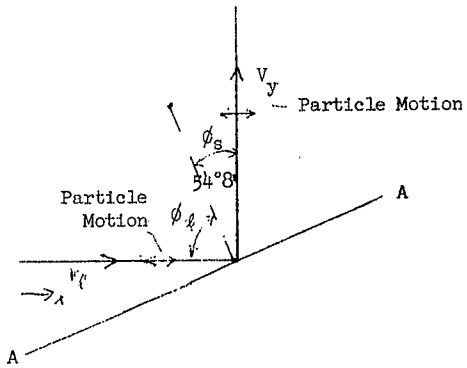
Figure 14. Reflection in x-y Plane
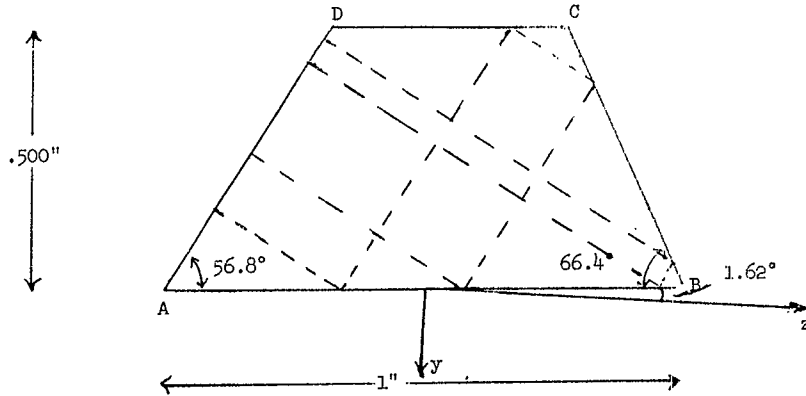
Figure 15. Test Block for x-shear Mode
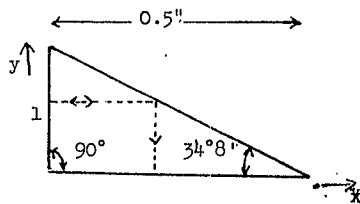
Figure 16. Test Block for x-y Plane Modes

20 μsec/cm

10 μsec/cm

5 μsec/cm
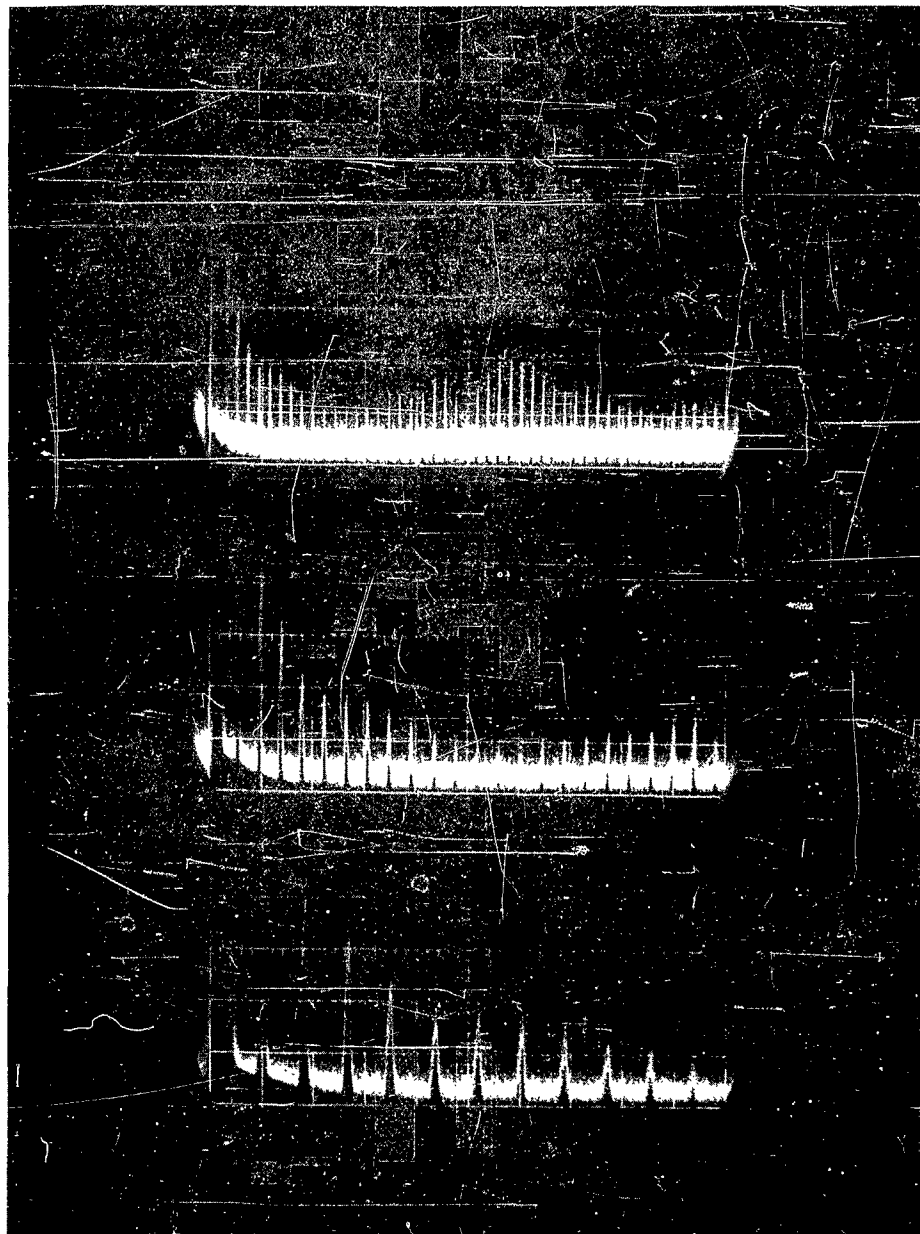
Figure 17.   Echoes in < 111 > Silicon at 1-3 gcps, 4°K
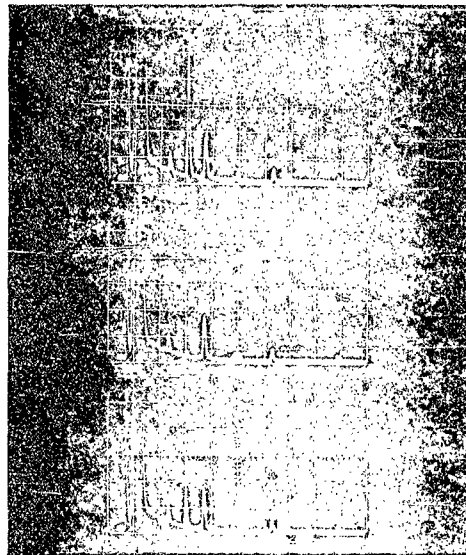
Pulses at 3rd and 5th cm. line
marking are of the fast trans-
verse mode. Time scale is
10 usec/cm.

Microscope light intensity is
applied. Echoes reduce very
rapidly.

110 volts d.c. bias applied
Echo reappears to height about
1/3 of its original magnitude.

Electron Phonon Interaction In GaAs

Crystal $\langle 110 \rangle$ GaAs   1.140" x .158" x .665"
Frequency   1.15 kMc/s
Transducer   Magnetostrictive films
Temperature   Liquid helium
Mode   Transverse 3.56 x 10^5 cm/sec.
Delay   9.5 usec. for round trip

Figure 18.

2 μsec/cm

5 μsec/cm
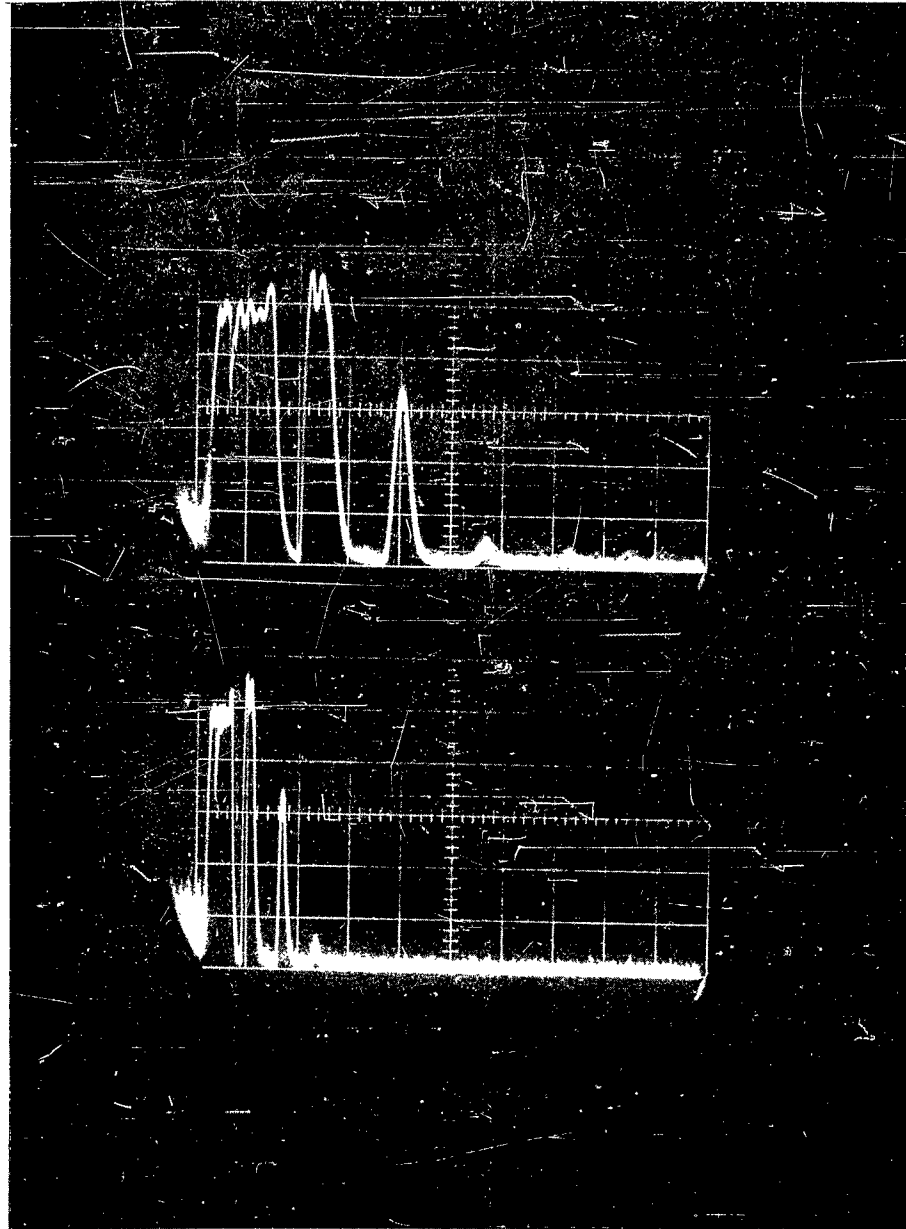
Figure 19.   Echoes in C Axis Ruby at 1-15 gcps, 300°K